Supplementary Material: Probabilistic patterns of interaction: The effects of link-strength variance on food-web structure

Justin D. Yeakel[1,*], Paulo R. Guimarães Jr[2], Mark Novak[3], Kena Fox-Dobbs[4], and Paul L. Koch[5]

[1]*Department of Ecology and Evolutionary Biology, University of California, Santa Cruz 1156 High St., Santa Cruz, CA 95064, USA*

[2]*Departamento e Ecologia Universidade de São Paulo, 05508-900, São Paulo, SP, Brazil*

[3]*Department of Zoology, Long Marine Laboratory, 100 Shaffer Rd, Santa Cruz, CA 95064, & Oregon State University, 3029 Cordley Hall, Corvallis, OR 97331, USA*

[4]*Department of Geology, University of Puget Sound, 1500 North Warner Street, CMB 1048, Tacoma, WA 98416, USA*

[5]*Department of Earth and Planetary Sciences, University of California, Santa Cruz, 1156 High St., Santa Cruz, CA 95064, USA*

J. R. Soc. Interface 1–21; doi: 10.1098/rspa.00000000

1. Appendix S1: Assessing structure from the NLID

Several structural properties were quantified for each of the three empirical food-webs (see Appendix S2). Primary among these were nestedness ($\mathcal{N}$; figure 1*a*) and modularity ($\mathcal{M}$; figure 1*b*), because these properties are thought to have important ramifications for the dynamics of ecological systems [1, 2, 3]. To quantify nestedness, we use the NODF (Nestedness based on Overlap and Decreased Fill) metric [4], where a value of 0 denotes an un-nested network and a value of 1 denotes a fully nested network.

Modularity has traditionally been quantified as the local density of links in a network [5], although other metrics exist [6]. Because our predator-prey networks have two trophic levels, we use the density of squares to estimate the average local link density [7]. A 'square' occurs when four nodes are connected by at least four links, and the average density of squares ($\bar{\rho}_s$) equals the number of squares in a network divided by the number of potential squares in a completely connected network, i.e. the local link density. This metric has the advantage of being analytically tractable for any network size, whereas other metrics use optimization methods [6]. As the connectance, C, of a network increases ($C = l/mn$, where l is the number of links in a network, and m and n are the number of prey and predator species, respectively), the local link density increases. We calculate modularity as

$$\mathcal{M} = \frac{\bar{\rho}_s - C}{\bar{\rho}_s + C}. \tag{1.1}$$

If the average local link density becomes greater than the overall link density, $\mathcal{M} \to +1$; if the average local link density becomes less than the overall link density, $\mathcal{M} \to -1$ (cf. [8]).

In addition to nestedness and modularity, we also quantified: 1) The frequency of networks characterized by low local link density ($\mathcal{M} = -1$; figure 1*b*); 2) the number of isolated components in a network, defined by disconnected subgraphs, each with ≥ 2 connected species (figure 1*c*); 3) the number of isolated species

in a network (figure 1*c*); and 4) the frequencies of four-species subgraphs (subunits of 2 predators connecting 2 prey) of which there are seven possible arrangements (figure 1*d*). The quantification of these six structural features (nestedness and modularity in addition to the four itemized structures) permits a holistic description of interaction patterns within a predator-prey network that, as a whole, can be used to compare the structural similarity of independent communities.

We assessed the ability of network models derived from NLIDs, with identical forbidden link structures as the empirical systems, to predict the six structural properties of empirical predator-prey networks. Predictive ability was scored by a similarity index (s_i) which varies between 1 (absolute similarity) and 0 (absolute dissimilarity) across cutoff values i (see Appendix S2 for details). We tested whether a good empirical parameterization of the NLID was enough to predict the general structure of empirical predator-prey networks. If so, then detailed quantification of strength variation within-links (PIDs) would not be necessary to characterize network structure. We varied the NLID standard deviation (SD) of our model networks towards higher and lower values than that measured from the empirical network, altering NLID shape. We then measured the structural similarity of empirical networks against models drawn from the NLID with altered SDs. If the NLID is strongly predictive of the empirical network structure, we expected a maximum value of s_i averaged across cutoffs i ($\bar{s}_{\max}$) when the model networks are drawn from the NLID matching that of the empirical network (figure 2*a*-*c*). This would suggest that the NLID encodes some structural properties of the empirical system. By extension, it would indicate that the empirical network structure is - in part - as would be predicted if species interactions were not organized by ecological tradeoffs. The effects of individual network properties can contribute to empirical and model network similarity differently. We show in figure 4 (main article) that nestedness tends to increase similarity ($\Delta\mathcal{N}$ values closer to 0), while modularity tends to decrease similarity ($\Delta\mathcal{M}$ values farther from 0).

As the shape of the model NLID is altered by changing its SD relative to the empirical SD, the effects on the underlaying patterns of interaction are not straightforward. To understand how structural variation affects these patterns, we explored how dietary unevenness varies as the shape of the NLID is altered. Dietary unevenness describes consumers connected by strong link-strengths to a small subset of available prey, and dietary evenness describes consumers connected by weaker link-strengths to a greater proportion of available prey (see Appendix S3 for details). Dietary unevenness can be used to measure the degree of specialization among consumers. However, if prey abundance is strongly skewed, even a predator without prey preferences (a generalist consumer) would look strongly uneven, incorrectly suggesting specialization. As a consequence, dietary unevenness cannot be compared among predators that consume prey with different abundances. Here we compare consumer dietary unevenness across the same set of prey within each site, which is equivalent to dietary specialization among sympatric consumers. We measured the degree of specialization for consumers in empirical and NLID-derived food-webs as the SD of the NLID was varied (figure 2*d-f*).

Both Saskatchewan and Amboseli had highest similarity when the model standard deviation matched the empirical NLID SD (NLID SD = 0.27 for both systems; $\bar{s}_{\max} = 0.93$ and 0.95 for Saskatchewan and Amboseli, respectively; figure 2*a,b*). The $\bar{s}_{\max}$ for Lake Naivasha was associated with a higher NLID SD than predicted by the empirical food-web (SD = 0.18, $\bar{s}_{\max} = 0.96$), however this value is not significantly different from the $\bar{s}$ for the empirical standard deviation (SD = 0.16, $\bar{s} = 0.95$; Welch's two sample t-test (df = 7.9): t = -0.17, $p = 0.86$; figure 2*c*). The sensitivity analysis revealed that NLID-based networks that share the same forbidden link structure have a high degree of structural similarity to empirical predator-prey networks. Furthermore, we found that similarity is strongly sensitive to the accurate parameterization of the NLID. This pattern holds across most cutoff values, especially when both weak and strong links of

the network were considered (i.e. low cutoff values) (figure 2*a-c*). By contrast, when only strong links (higher cutoff values) were considered, SDs higher than the empirical SD were equally suitable for reproducing structure observed in the empirical networks.

The shape of the NLID had a large impact on the degree of dietary specialization among consumers (figure 2*d-f*), though the relationship is nonlinear; low NLID SD leads to model networks dominated by generalists, while high SD leads to model networks dominated by moderate to strong specialists. Model networks matching the SD of the empirical NLID (maximum similarity between the model and empirical networks) resulted in intermediate values. Furthermore, an analysis of specialization among consumers revealed higher values than expected compared to model networks. This underestimate indicates that Saskatchewan and East African predators have stronger prey preferences than expected from model networks. Moreover, saturation of $\bar{s}_i$ at high SD for the strongest links in the networks ($i = 0.4, 0.5$) suggests that structure collapses similarly for empirical and model systems when specialist consumers dominate. This indicates that 1) the inclusion of weaker links in the system has a disproportionate impact on structure, particularly when the food-web is dominated by specialists, and 2) the structures imparted by the strongest links are not different from those generated by random processes and are less sensitive to NLID shape. Importantly, our results show that much of the structure of these predator-prey networks is predictable from link-strength variance at the level of the system. This means that the variance in strength among links in a predator-prey network, without regard to the specific and unique interactions among species, strongly influences structure. Whether models derived from the NLID accurately predict specific structures such as nestedness or modularity is not known.

2. Appendix S2: Isotopic systems and mixing model results

We used the isotopic values of predators and prey from three systems: one from Saskatchewan, Canada (figure S3, [9]), and two from Kenya: Amboseli (figure S4, [10]), and Lake Naivasha (figure S5 [11]). To calculate distributions of the contribution of each prey to a predator's diet, we first accounted for trophic discrimination factors, such that isotopic fractionations that occur between trophic levels are eliminated. For both African systems, predator δ^{13}C and δ^{15}N values were corrected by -1 ± 0.5‰ and -3.5 ± 0.7‰ respectively, thereby assuming that all carnivores had high-quality protein-rich diets [12, 13, 14]. For Saskatchewan, Canada, predator δ^{13}C and δ^{15}N values were corrected by -1.3 ± 0.5‰ and -4.5 ± 0.7‰ respectively, more closely matching values calculated by [15] in the wolf-moose-beaver Isle Royale system. This differs from the discrimination factors used by [9].

We corrected for potential underestimates of isotopic variance for predators with low sample sizes by incorporating variance measurements for the same species in nearby systems. Measures of variance for hyenas and cheetahs in southern Kenya (unpublished data) were used as more conservative estimates of variance for the same species in Amboseli. Similarly, measures of variance for lions, leopards, and cheetah from central and southern Kenya (unpublished data) were used as more conservative estimates of variance for the same species in Lake Naivasha (final values are reported in table 1). The means and standard deviations presented are similar to the isotopic values of the same species from other African systems [16, 17]. In this manner, variance for under-sampled predators was increased, conservatively increasing the uncertainty represented in the posterior probability distributions calculated by mixSIR.

Link-strength distributions were assessed for predator:prey pairs in all systems (with the isotope mixing model MixSIR v.1.0.4 [18]; figure S3,4) with the exception of the Naivasha food-web where some browsers with very low δ^{13}C values were too isotopically similar to resolve dietary information [11] and were

binned as a functional group (figure S5). Because these browsers had isotopic values that differed significantly from all predators in the system, binning does not significantly influence the estimation of interaction distributions for their primary prey.

3. Appendix S3: Calculation of Similarity and Specialization

The application of the cutoff algorithm to both the empirical and model food-webs results in a series of vectors $\mathbf{v}_i$ that describe the topological properties of food-webs represented in the ensemble across each of the i cutoff values. The elements of both vectors are defined by values for: nestedness, modularity, the proportion of networks with positive connectance but no squares (where a square is formed by connecting four nodes with four links), the number of single nodes, the number of components, and the frequencies of each four-node motif. All elements in a vector are normalized to vary between 0 and 1 (except for modularity, which can vary between -1 and 1), thus limiting each element of the vector to a standardized range. We emphasize that the elements of these vectors were chosen arbitrarily (other structural properties of networks could be included as well), such that the absolute similarity between two food-webs should be assessed relative to other food-webs measured with the same indices included in the similarity index. The degree to which a model food-web predicts the structural properties of an empirical food-web can be quantified with a similarity coefficient

$$s_i = \frac{\mathbf{v}_{i,\text{empirical}} \cdot \mathbf{v}_{i,\text{model}}}{|\mathbf{v}_{i,\text{empirical}}||\mathbf{v}_{i,\text{model}}|}, \tag{3.1}$$

where $\mathbf{v}_{i,\text{empirical}}$ and $\mathbf{v}_{i,\text{model}}$ are vectors of topological metric values corresponding to a cutoff value $i \in \{0.1 : 0.5\}$ for the empirical and model networks, respectively, and $|\cdot|$ denotes the euclidean norm for the given vector [19, 20]. The similarity index s_i can vary between 0 and 1; a value of 0 indicates absolute dissimilarity, while a value of 1 indicates absolute similarity. We note

that this similarity index is mathematically related to the cosine of the angle between two vectors. To assess the similarity of network ensembles, rather than a single network, we bootstrapped 1000 network vectors from both the empirical and model ensembles, thereby generating a distribution of similarity values that represent the topological equivalency between the empirical and model probabilistic food-webs.

Calculation of Consumer Dietary Specialization

The degree of consumer dietary unevenness, or specialization (ϵ) can be directly calculated from the mixing model results of a consumer's isotopic values (relative to those of its prey). We first define a consumer dietary vector that has equally-weighted prey contribution-to-diet links as an generalist consumer end-member ($\gamma = \{1/n, ..., 1/n\}$, where n is the number of potential prey, and where the sum of the vector equals unity), and a consumer with only a single link to one of its potential prey as a specialist consumer end-member ($\phi = \{1, 0, ..., 0\}$). In n-dimensional diet-space, where n represents the number of potential prey, we define the centroid by the generalist consumer. The Euclidean distance of a given consumer's diet to the centroid can then be measured. We divide this distance by the Euclidean distance from the centroid to the specialist consumer end-member such that consumers with different numbers of prey can be directly compared (Eq. 3.2). Thus, consumer dietary unevenness of a consumer j can be quantified by

$$\epsilon_j = \frac{\sqrt{\sum_{k=1}^{n}(w_{jk} - \gamma_{jk})^2}}{\sqrt{\sum_{k=1}^{n}(\phi_{jk} - \gamma_{jk})^2}}, \tag{3.2}$$

where the subscript k refers to a prey item in the diet of the consumer j. Consumer dietary specialization is therefore constrained to vary between 0 and 1, where 0 represents a maximally generalist consumer, and 1 represents a maximally specialist consumer. We note that the use of entropy-based unevenness measurements [21, 22] result in similar estimates.

References

1 Thébault, E., Fontaine, C. 2010 Stability of Ecological Communities and the Architecture of Mutualistic and Trophic Networks. *Science.* **329**, 853-856.

2 Kondoh, M., Kato, S., Sakato, Y. 2010 Food webs are built up with nested subwebs. *Ecology.* **91**, 3123-3130.

3 Stouffer, D. B., Bascompte, J. 2011 Compartmentalization increases food-web persistence. *Proc. Natl. Acad. Sci. USA.* **108**, 3648-3652.

4 Almeida-Neto, M., Guimarães, P., Guimarães Jr, P. R., Loyola, R. D., Ulrich, W. 2008 A consistent metric for nestedness analysis in ecological systems: reconciling concept and measurement. *Oikos.* **117**, 1227-1239.

5 Camacho, J., Guimerà, R., Nunes Amaral, L. A. N. 2002 Robust patterns in food web structure. *Phys. Rev. Lett.* **88**, 228102-1-228102-4.

6 Guimerà, R., Amaral, L. A. N. 2005 Cartography of complex networks: modules and universal roles. *J. Stat. Mech.* **2005**, P02001.

7 Zhang, P., Wang, J., Li, X., Li, M., Di, Z., Fan, Y. 2008 Clustering coefficient and community structure of bipartite networks. *Physica A.* **387**, 6869–6875.

8 Araújo, M. S., Guimarães Jr, P. R., Svanback, R., Pinheiro, A., Guimarães, P., Reis, S. F., et al. 2008 Network analysis reveals contrasting effects of intraspecific competition on individual vs. population diets. *Ecology.* **89**, 1981-1993.

9 Urton, E. J. M., Hobson, K. A. 2005 Intrapopulation variation in gray wolf isotope (δ^{15}N and δ^{13}C) profiles: implications for the ecology of individuals. *Oecologia.* **145**, 317-326.

10 Koch, P. L., Behrensmeyer, A. K. 1990 The isotopic ecology of plants and animals in Amboseli National Park, Kenya. Annual Report to the Director.

11 Ambrose, S. H., DeNiro, M. J. 1986 The isotopic ecology of East African mammals. *Oecologia.* **69**, 395-406.

12 Roth, J. D., Hobson, K. A. 2000 Stable carbon and nitrogen isotopic fractionation between diet and tissue of captive red fox: implications for dietary reconstruction. *Can. J. Zool.* **78**, 848-852.

13 Robbins, C. T., Felicetti, L. A., Sponheimer, M. 2005 The effect of dietary protein quality on nitrogen isotope discrimination in mammals and birds. *Oecologia.* **144**, 534-540.

14 Robbins, C. T., Felicetti, L. A., Florin, S. T. 2010 The impact of protein quality on stable nitrogen isotope ratio discrimination and assimilated diet estimation. *Oecologia.* **162**, 571-579.

15 Fox-Dobbs, K, Bump, J. K., Peterson, R. O., Fox, D. L., Koch, P. L. 2007 Carnivore-specific stable isotope variables and variation in the foraging ecology of modern and ancient wolf populations: case studies from Isle Royale, Minnesota, and La Brea. *Can. J. Zool.* **85**, 458-471.

16 Codron, D., Codron, J., Lee-Thorp, J. A., Sponheimer, M., Ruiter, D., Brink, J. S. 2007 Stable isotope characterization of mammalian predator–prey relationships in a South African savanna. *Eur. J. Wildlife Res.* **53**, 161-170.

17 Yeakel, J. D., Patterson, B. D., Fox-Dobbs, K., Okumura, M., Cerling, T., Moore, J., et al. 2009 Cooperation and individuality among man-eating lions. *Proc Natl Acad Sci USA.* **106**, 19040-19043.

18 Moore, J. W., Semmens, B. X. 2008 Incorporating uncertainty and prior information into stable isotope mixing models. *Ecol. Lett.* **11**, 470-480.

19 Kohn, A., Riggs, A. 1982 Sample Size Dependence in Measures of Proportional Similarity. *Mar. Ecol.-Prog. Ser.* **9**, 147-151.

20 Smith, E., Pontasch, K., Cairns, J. 1990 Community similarity and the analysis of multispecies environmental data: a unified statistical approach. *Water Res.* **24**, 507-514.

21 Keylock, C. 2005 Simpson diversity and the Shannon–Wiener index as special cases of a generalized entropy. *Oikos.* **109**, 203-207.

22 Blüthgen, N., Menzel, F., Blüthgen, N. 2006 Measuring specialization in species interaction networks. *BMC Ecol.* **6**, 9.

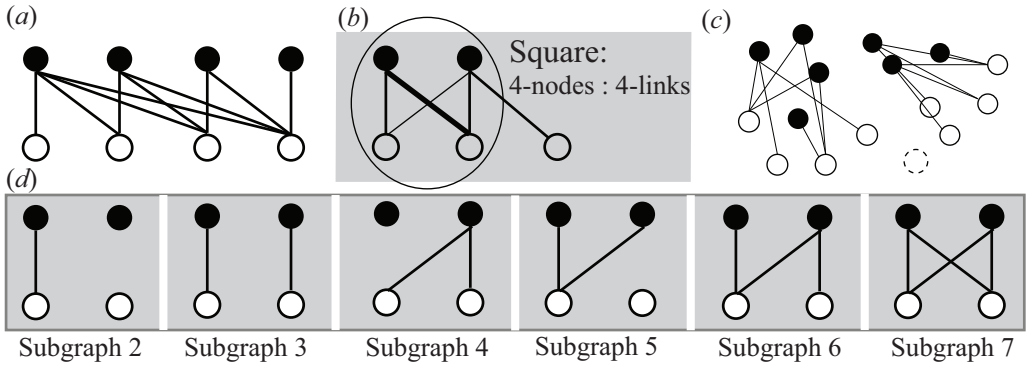

Figure S 1. (*a*) A nested pattern of interaction, where the consumers (black circles) towards the right consume prey (white circles) that are subsets of the consumers towards the left. (*b*) A network square (circled), with four nodes connected to four links. Modularity is both a function of the average density of squares relative to a fully connected network, and network connectance. In this example, at high cutoff values, the density of squares $\rightarrow 0$, while connectance > 0, resulting in a modularity value of -1 (see Eq. 1.1). (*c*) Two network components and an isolated node (stippled). (*d*) Network Subgraphs 2 through 7. Subgraph 1 is represented by 2 predators and 2 prey not connected by interactions (not shown).

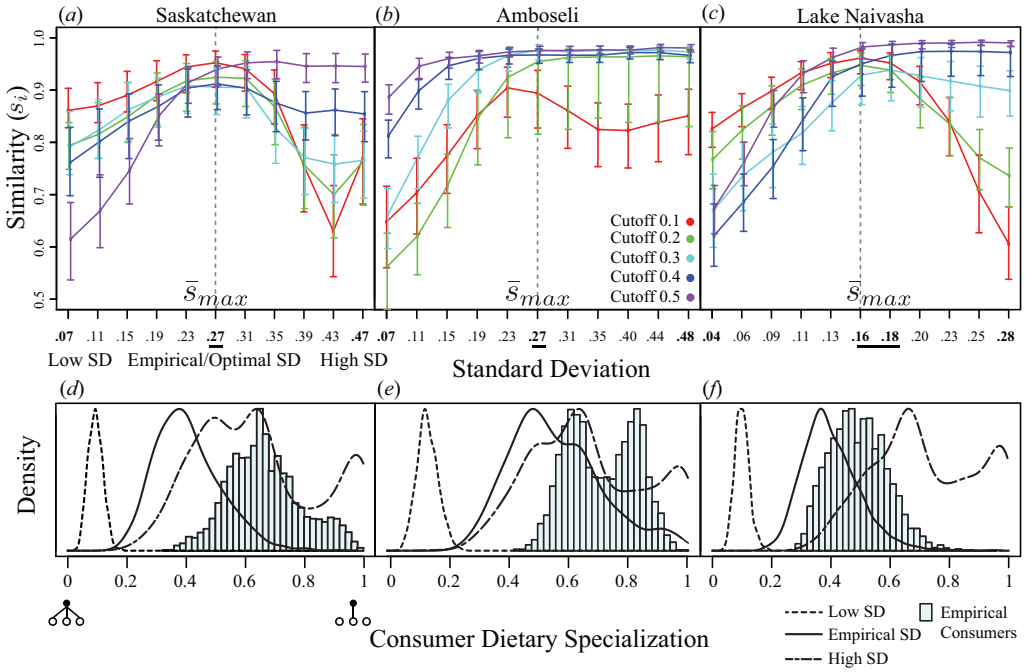

Figure S 2. (*a-c*) Sensitivity analyses of the Saskatchewan, Amboseli, and Lake Naivasha food-web ensembles, respectively. Similarity values are on the y-axis, and the x-axis ranges from a lower standard deviation (SD) than the empirical SD to a higher SD (stippled line denotes the empirical SD). Curves describe median similarity values for each cutoff (legend), and whiskers denote 25$^{\text{th}}$ and 75$^{\text{th}}$ percentiles. Underlined values mark the SD with highest average similarity. (*d-f*) Consumer specialization for low, empirical, and high SD, and for Saskatchewan, Amboseli, and Naivasha consumers, respectively. When NLID SD is low, generalists dominate. When NLID SD is high, specialists dominate. When NLID SD is equivalent to the empirical value, intermediate consumers dominate.

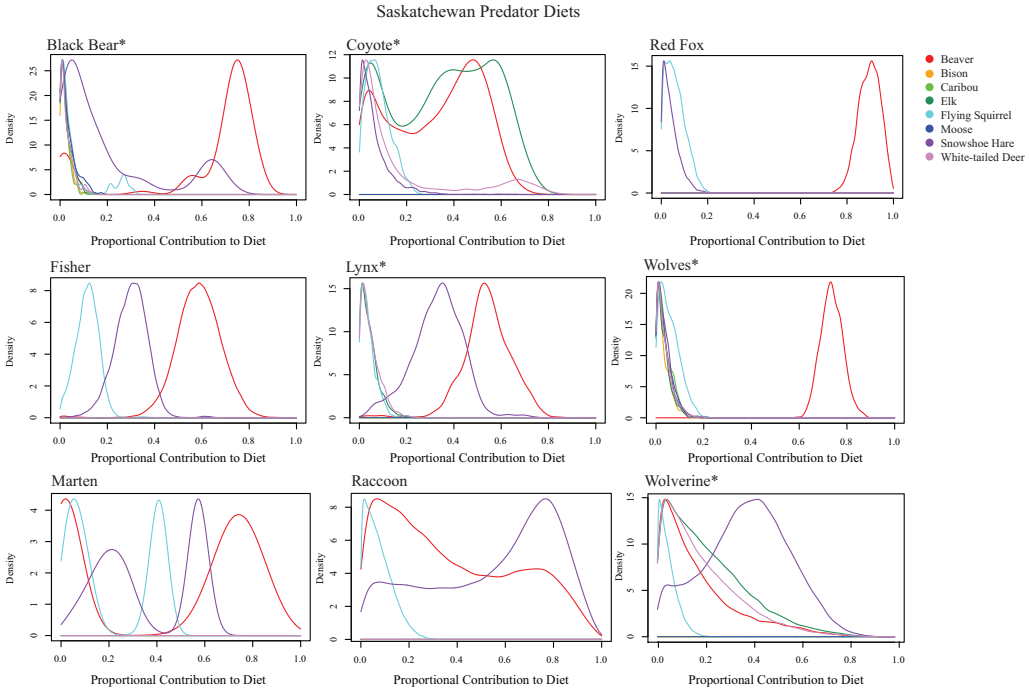

Figure S 3. Proportional contribution of prey to the diet of predators (PIDs) in the Saskatchewan system. PID estimates are from the Bayesian isotope mixing model MixSIR. Predator:prey PIDs that are not reported indicate the presence of a forbidden interaction. Species marked with stars represent the larger predators in the system; topological properties were assessed with just these predators included, and are reported in figure S6. Forbidden Links: Fox, fisher, marten, and raccoon to bison, caribou, elk, moose, white-tailed deer; coyote, lynx, and wolverine to bison, caribou, moose.

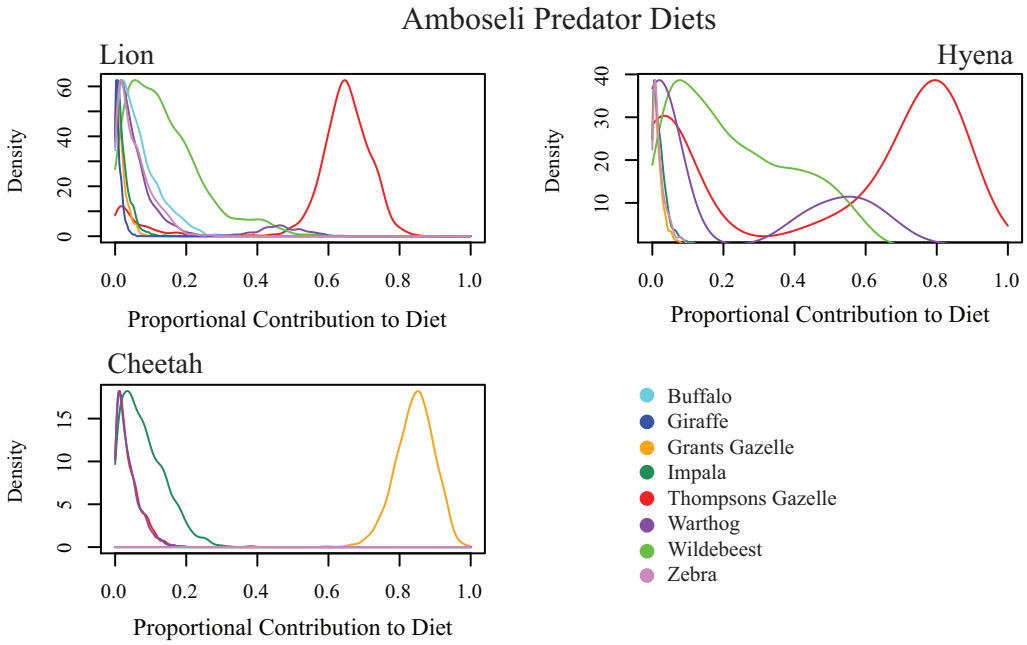

Figure S 4. Proportional contribution of prey to the diet of predators (PIDs) in the Amboseli system. PID estimates are from the Bayesian isotope mixing model MixSIR. Predator:prey PIDs that are not reported indicate the presence of a forbidden link. Forbidden Links: cheetah to buffalo, giraffe, wildebeest, zebra.

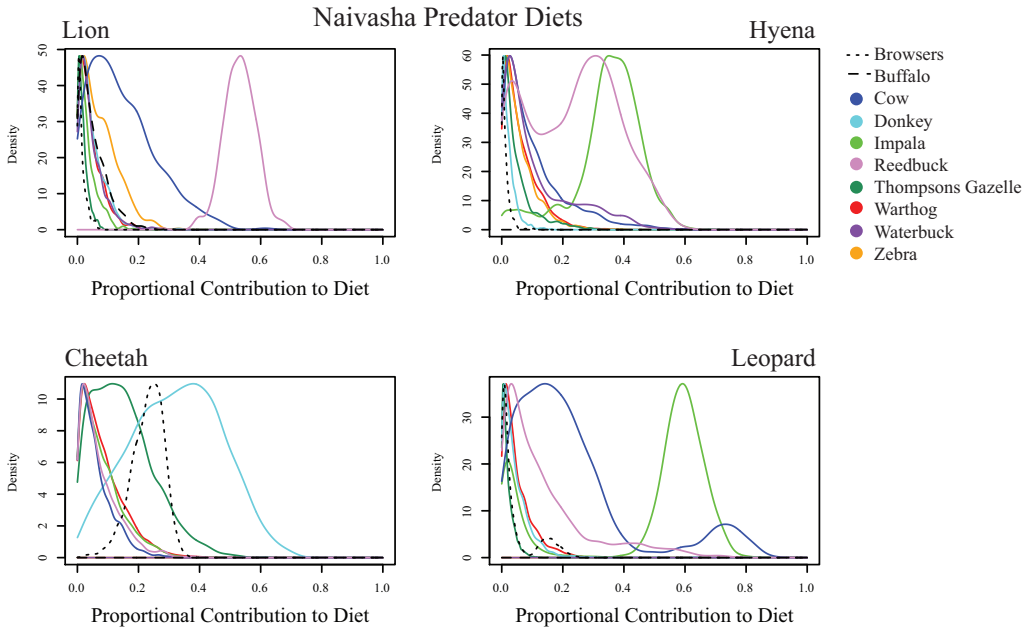

Figure S 5. Proportional contribution of prey to the diet of predators (PIDs) in the Naivasha system. PID estimates are from the Bayesian isotope mixing model MixSIR. Predator:prey PIDs that are not reported indicate the presence of a forbidden link. A subset of browsers were too isotopically similar to resolve dietary information, though they had values set apart from all potential predators, suggesting minimal dietary inclusion. As such, they were binned together as a 'browser' functional group and include: Steenbok, Dik Dik, Baboon, Grey Duiker, Klipspringer, Bushbuck, and Eland. Forbidden Links: cheetah and leopard to buffalo, waterbuck, and zebra.

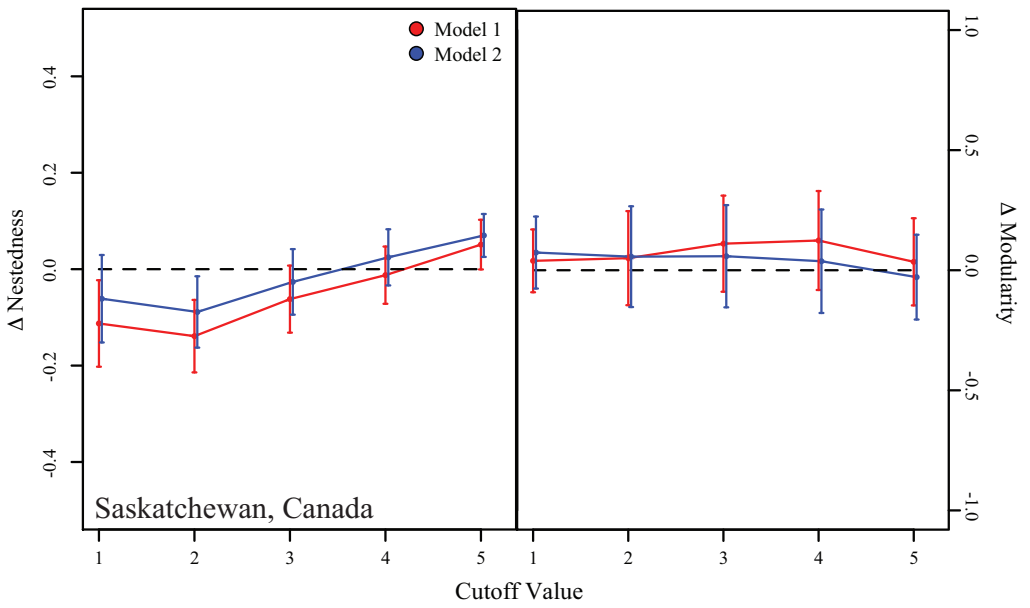

Figure S 6. The difference (Δ) in nestedness (empirical - model values) for Saskatchewan, Canada, with only the large predators (and predators that primarily consume larger prey) included in the food-web ensemble. Predators include: Black bear, Coyote, Lynx, Wolves, and Wolverine. These results are qualitatively similar to those obtained for the full food-web, suggesting that the structure of interactions is fairly robust to modification. Red: Model 1; Blue: Model 2.

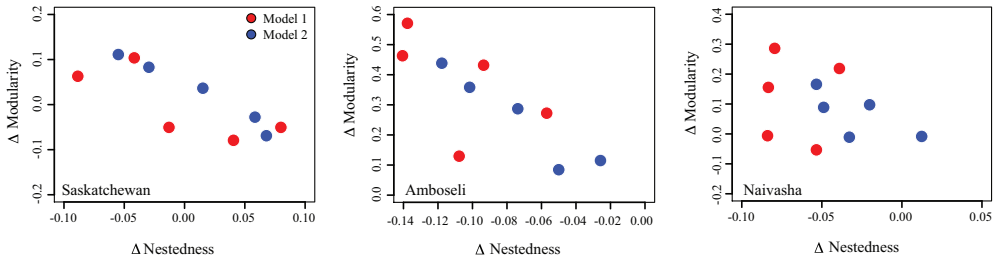

Figure S 7. The difference (Δ) in modularity (empirical - model values) vs. the difference in nestedness for the three isotopic food-webs. Each point corresponds to a measurement of nestedness and modularity for cutoff values 0.1 to 0.5. Model 1 does not incorporate body size constraints, while Model 2 does incorporate body size constraints. In each system, there is a strong negative relationship between modularity and nestedness for Model 2 (though this relationship is not statistically significant for the Naivasha system). Saskatchewan Model 1: $R^2 = 0.47$, $p > 0.05$, Model 2: $R^2 = 0.96$, $p \ll 0.05$. Amboseli Model 1: $R^2 = 0.09$; $p > 0.05$, Model 2: $R^2 = 0.86$; $p < 0.05$. Naivasha Model 1: $R^2 = -0.33$; $p > 0.05$, Model 2: $R^2 = 0.25$; $p > 0.05$.

Species	δ^{13}C	δ^{13}C SD	δ^{15}N	δ^{15}N SD
Amboseli				
Panthera leo	-9.04	1.67	11.07	0.45
Crocuta crocuta	-9.16	0.89	12.16	1.09
Acinonyx jubatus	-17.21	1.95	10.07	1.02
Naivasha				
Panthera leo	-7.21	1.64	6.30	0.44
Crocuta crocuta	-8.74	0.89	7.70	1.10
Panthera pardus	-8.61	0.51	6.70	2.04
Acinonyx jubatus	-14.21	1.95	6.60	1.02

Table S 1. Mean and standard deviations (SDs) of isotopic values for African predators and prey that were used to assess link-strengths with the Bayesian isotope mixing model MixSIR. See Appendix S1 for details.

System size range (# links)	a	b
Mean Error		
1:100	0.06	3.02
101:200	0.05	3.88
201:300	0.05	4.24
301:400	0.04	4.74
401:500	0.04	5.19
SD Error		
1:100	0.09	2.86
101:200	0.08	3.87
201:300	0.07	4.30
301:400	0.06	4.57
401:500	0.06	5.06

Table S 2. To determine the rate at which estimation of the mean and standard deviation (SD) of the NLID could be estimated as sampling effort increased, exponential curves ($y = ae^{bx}$) were fitted to binned numerical results, where each bin represents an increase in ecosystem size by 100 links. Mean error and SD error were calculated as the difference between the true NLID mean and SD, respectively, and that estimated from subsampling PIDs.

$\Delta\mathcal{N}$	Saskatchewan			Amboseli			Naivasha		
Cutoff	df	t	p	df	t	p	df	t	p
0.1	57.7	-0.62	0.54	57.9	-3.87	$< 0.01^*$	57.9	-4.08	$< 0.01^*$
0.2	51.7	-1.97	0.05	54.8	-0.507	0.61	57.2	-0.68	0.52
0.3	57.9	-1.31	0.20	53.9	-2.53	0.01^*	55.2	-1.81	0.07
0.4	55.9	-2.35	0.02^*	56.6	-0.06	0.95	57.0	-2.24	0.03^*
0.5	56.8	1.44	0.16	48.3	-2.60	0.01^*	57.4	-1.57	0.12
$\Delta\mathcal{M}$	Saskatchewan			Amboseli			Naivasha		
Cutoff	df	t	p	df	t	p	df	t	p
0.1	53.0	2.25	0.03^*	57.4	1.44	0.16	54.4	-1.49	0.14
0.2	57.9	-0.05	0.96	48.6	-0.61	0.55	57.0	1.21	0.23
0.3	45.1	-1.63	0.11	57.6	3.30	$< 0.01^*$	57.9	0.25	0.81
0.4	57.2	-0.63	0.53	56.2	1.55	0.13	52.7	2.70	$< 0.01^*$
0.5	50.8	-1.02	0.31	52.2	4.49	$\ll 0.01^*$	54.3	3.20	$< 0.01^*$

Table S 3. Welch t-test results for $\Delta\mathcal{N}$ and $\Delta\mathcal{M}$ between Models 1 and 2. Model 1 does not include body size constraints, while Model 2 does include body size constraints (refer to figure 6, main text). For the most part, the mean values of Model 1 and 2 are not significantly different, with some exceptions indicated by the asterisk (*).